THE ASTRONOMICAL JOURNAL, 119:292–301, 2000 January

HST/WFPC2 AND VLT/ISAAC OBSERVATIONS OF PROPLYDS IN THE GIANT H II REGION NGC 3603[1]

WOLFGANG BRANDNER,[2] EVA K. GREBEL,[3,4] YOU-HUA CHU,[5] HORACIO DOTTORI,[6] BERNHARD BRANDL,[7] SABINE RICHLING,[8,9] HAROLD W. YORKE,[8] SEAN D. POINTS,[5] AND HANS ZINNECKER[10]
Received 1999 September 4; accepted 1999 September 27

ABSTRACT

We report the discovery of three proplyd-like structures in the giant H II region NGC 3603. The emission nebulae are clearly resolved in narrowband and broadband *HST*/WFPC2 observations in the optical and broadband VLT/ISAAC observations in the near-infrared. All three nebulae are tadpole shaped, with the bright ionization front at the head facing the central cluster and a fainter ionization front around the tail pointing away from the cluster. Typical sizes are 6000 AU × 20,000 AU The nebulae share the overall morphology of the proplyds (PROto PLanetarY DiskS) in Orion, but are 20 to 30 times larger in size. Additional faint filaments located between the nebulae and the central ionizing cluster can be interpreted as bow shocks resulting from the interaction of the fast winds from the high-mass stars in the cluster with the evaporation flow from the proplyds. Low-resolution spectra of the brightest nebula, which is at a projected separation of 1.3 pc from the cluster, reveal that it has the spectral excitation characteristics of an ultra compact H II region with electron densities well in excess of 10^4 cm^{-3}. The near-infrared data reveal a point source superposed on the ionization front. The striking similarity of the tadpole-shaped emission nebulae in NGC 3603 to the proplyds in Orion suggests that the physical structure of both types of objects might be the same. We present two-dimensional radiation hydrodynamical simulations of an externally illuminated star-disk-envelope system, which was still in its main accretion phase when first exposed to ionizing radiation from the central cluster. The simulations reproduce the overall morphology of the proplyds in NGC 3603 very well, but also indicate that mass-loss rates of up to 10^{-5} $M_\odot$ yr^{-1} are required in order to explain the size of the proplyds.

Due to these high mass-loss rates, the proplyds in NGC 3603 should only survive $\approx 10^5$ yr. Despite this short survival time, we detect three proplyds. This indicates that circumstellar disks must be common around young stars in NGC 3603 and that these particular proplyds have only recently been exposed to their present harsh UV environment.

Key words: circumstellar matter — stars: formation — stars: pre–main-sequence — open clusters and associations: individual (NGC 3603) — ISM: individual (NGC 3603)

1. INTRODUCTION

HST/WFPC2 observations of the Orion Nebula (M42) revealed a large variety of dark silhouette disks (O'Dell & Wong 1996; McCaughrean & O'Dell 1996) and partially ionized circumstellar clouds (O'Dell, Wen, & Hu 1993). Many of the circumstellar clouds, which had first been detected from the ground by Laques & Vidal (1979), have a cometary shape with the tails pointing away from the O7V star Θ^1 Ori C and the O9.5V star Θ^2 Ori A, the brightest and most massive members of the Trapezium cluster. The partially ionized circumstellar clouds with cometary shape were identified as protoplanetary disks (proplyds) around young stars, which are ionized from the outside (Churchwell et al. 1987; O'Dell et al. 1993).

Many proplyds are ionization bounded, which indicates that all EUV photons ($h\nu \geq 13$ eV) get absorbed in the ionization front engulfing the protostar and its circumstellar disk (O'Dell 1998). FUV photons (13 eV $> h\nu \geq 6$ eV), however, are able to penetrate the ionization front. They heat up the inside of the proplyd envelope and lead to the dissociation of molecules in the outer layers of the circumstellar disk (Johnstone, Hollenbach, & Bally 1998). The resulting evaporation flow provides a steady supply of neutral atoms to the ionization front and leads to the development of a cometary tail (McCullough et al. 1995; Störzer & Hollenbach 1999).

Because of their larger size and the ionized envelope, proplyds can be spotted more easily than circumstellar disks themselves. Consequently, Stecklum et al. (1998) proposed utilizing proplyds as tracers for circumstellar disks in distant star-forming regions. Systematic search efforts for proplyds in H II regions around young clusters with WFPC2 did not yield any new detections (Stapelfeldt et al.

[1] Based on observations obtained at the European Southern Observatory, Paranal and La Silla (ESO proposals 47.5-0011, 53.7-0122, 58.E-0965, 59.D-0330, 63.I-0015) and on observations made with the NASA/ESA *Hubble Space Telescope*, obtained from the Space Telescope Science Institute. STScI is operated by the Association of Universities for Research in Astronomy, Inc., under NASA contract NAS 5-26555.

[2] University of Hawaii, Institute for Astronomy, 2680 Woodlawn Drive, Honolulu, HI 96822; brandner@ifa.hawaii.edu.

[3] Department of Astronomy, University of Washington at Seattle, Box 351580, Seattle, WA 98195; grebel@astro.washington.edu.

[4] Hubble Fellow.

[5] Department of Astronomy, University of Illinois at Urbana-Champaign, 1002 West Green Street, Urbana, IL 61801; chu@astro.uiuc.edu, points@astro.uiuc.edu.

[6] Instituto de Física, UFRGS, Campos do Vale, C.P. 15051, 91500 Porto Alegre, R.S., Brazil; dottori@if.ufrgs.br.

[7] Department of Astronomy, Cornell University, 222 Space Sciences Building, Ithaca, NY 14853; brandl@astrosun.tn.cornell.edu.

[8] Jet Propulsion Laboratory, California Institute of Technology, 4800 Oak Grove Drive, Mail Stop 169-506, Pasadena, CA 91109; richling@ita.uni-heidelberg.de, Harold.Yorke@jpl.nasa.gov.

[9] Institut für Theoretische Astrophysik, Universität Heidelberg, Tiergartenstraße 15, D-69121 Heidelberg, Germany.

[10] Astrophysikalisches Institut Potsdam, An der Sternwarte 16, D-14482 Potsdam, Germany.

1997; Bally et al. 1998a). Until recently, only one other proplyd had been found. It is located in the vicinity of the O7V star Herschel 36 in the Lagoon Nebula (M16; Stecklum et al. 1998).

NGC 3603 is located in the Carina spiral arm at a distance of 6 kpc (De Pree, Nysewander, & Goss 1999 and references therein). With a bolometric luminosity $L_{\rm bol} > 10^7$ $L_\odot$, NGC 3603 is 100 times more luminous than the Orion Nebula and has about 10% of the luminosity of 30 Doradus in the Large Magellanic Cloud (LMC). It is the only Galactic giant H II region whose massive central ionizing cluster can also be studied at optical wavelengths. The initial mass function of the cluster follows a Salpeter-type power law with index $\Gamma = -1.70$ for masses greater than 25 $M_\odot$ and $\Gamma = -0.73$ for masses less than 25 $M_\odot$ (Eisenhauer et al. 1998), extending from Wolf-Rayet stars and O3V stars with masses up to 120 $M_\odot$ (Drissen et al. 1995) down to stars of at least 1 $M_\odot$ (Eisenhauer et al. 1998). The total cluster mass is $\geq 4000\ M_\odot$.

To the south of the cluster is a giant molecular cloud. Ionizing radiation and fast stellar winds from the starburst cluster are excavating large gaseous pillars. Located about 20″ to the north of the cluster center is the blue supergiant Sher 25. This supergiant is unique because its circumstellar ring and bipolar outflows form an hourglass structure similar to that of SN1987A (Brandner et al. 1997a, 1997b).

As part of a follow-up study on the hourglass structure around Sher 25 we observed NGC 3603 with *HST*/WFPC2. In this paper, we report the serendipitous discovery of three proplyd-like structures in NGC 3603 based on *HST*/WFPC2 and VLT/ISAAC observation and perform a first analysis of their physical properties.

2. OBSERVATIONS AND DATA REDUCTION

2.1. *HST/WFPC2 Observations*

On 1999 March 5 we obtained deep narrowband Hα (F656N, 2 × 500 s) and [N II] (F658N, 2 × 600 s) observations of the giant H II region NGC 3603. The Planetary Camera (PC) chip was centered on the bipolar outflow structure around the blue supergiant Sher 25. The three Wide Field Camera (WF) chips covered the central cluster and the H II region to the south of Sher 25.

In addition, we retrieved and analyzed archival *HST* data, which had originally been obtained in 1997 July (PI, L. Drissen). The PC was centered on the cluster, and the three WF chips covered the area northwest of the cluster. Using IRAF,[11] we combined individual short exposure in F547M (8 × 30 s), F675W (8 × 20 s), and F814W (8 × 20 s) to produce images with effective exposure times of 240 s, 160 s, and 160 s, respectively.

The surface brightness of the proplyds was measured using aperture photometry with an aperture radius of 0.″5. The photometric calibration was carried out following the steps outlined in the *HST* Data Handbook, Version 3. No attempt was made to correct for the contribution of the [N II] lines to the Hα F656N filter or the contribution of the Hα line to the [N II] F658N filter. The spectrum of proplyd 1 (see below) indicates that the underlying continuum emission from the proplyd is negligible. Applying equation (3) from O'Dell (1998) yields that the contribution of the [N II] lines to the total flux observed in the Hα F656N filter is at most 3.5%.

2.2. *Preparatory Ground-based Observations*

A first set of deep ground-based broad and narrowband images of NGC 3603 was obtained on 1991 April 22 with the ESO New Technology Telescope and the ESO Multi-Mode Instrument (EMMI). These data were used to identify a number of compact emission nebula in the vicinity of the central cluster.

On 1994 April 2 we tried to resolve the inner structure of the compact nebulae using the ESO Adaptive Optics system ADONIS. This attempt failed owing to the lack of sufficiently bright stars suitable for wave-front sensing within 20″ of any of the proplyds.

A low-dispersion spectrum of proplyd 1 was obtained on 1997 February 3 with the ESO/MPI 2.2 m telescope and the ESO Faint Object Spectrograph 2 (EFOSC2) at La Silla, Chile. The slit width was 1.″5. The spectrum has a sampling of 0.2 nm pixel^{-1}, a spectral resolution around 450 km s^{-1}, and covers the wavelength range from 517 nm to 928 nm. It was wavelength and flux calibrated using IRAF. We did not try to correct for fringes, which become noticeable redward of 750 nm.

2.3. *VLT/ISAAC Observations*

As part of a study of the low-mass stellar content of the starburst cluster (see Brandl et al. 1999), NGC 3603 was observed with the ESO Very Large Telescope (VLT) Unit Telescope 1 (UT1, now officially named ANTU) during the nights of 1999 April 4–6 and 9. The observations were carried out in service mode and used the Infrared Spectrograph and Array Camera (ISAAC; see Moorwood et al. 1998). Deep near-infrared observations of NGC 3603 were obtained with effective exposure times in J_s, H, and K_s of 2230 s, 2710 s, and 2890 s, respectively. The seeing (FWHM) on the co-added frames was of the order of 0.″35 to 0.″40. Dithering between individual exposures increased the field of view from its nominal value of 2.′5 × 2.′5 to 3.′5 × 3.′5. The data were flux calibrated based on observations of faint near-infrared standard stars from the lists by Hunt et al. (1998) and Persson et al. (1998).

More details on the data reduction and analysis can be found in Brandl et al. (1999).

3. PHYSICAL PROPERTIES OF PROPLYDS

3.1. *Morphology and Size*

The *HST*/WFPC2 observations are presented in Figure 1. The figure shows an overlay of two composite color images. The upper part of the image consists of the archive data with the following color coding: F547M (*blue*), F675W (*green*), F814W (*red*). Overlaid are our new WFPC2 data with the F656N data in the red channel, the average of F656N and F658N in the green channel, and F658N in the blue channel. The locations of the proplyds are marked by small boxes, and enlargements of the boxes are shown in the upper part of Figure 1. Proplyd 3 has only been observed in intermediate and broadband filters and thus stands out less clearly against the underlying background when compared to proplyds 1 and 2. The insert at the lower right shows a color composite of *HST*/WFPC2 F656N (*blue*) and F658N (*green*) data and VLT/ISAAC K_s data (*red*).

[11] IRAF is distributed by the National Optical Astronomy Observatories, which are operated by the Assocation of Universities for Research in Astronomy, Inc., under cooperative agreement with the National Science Foundation.

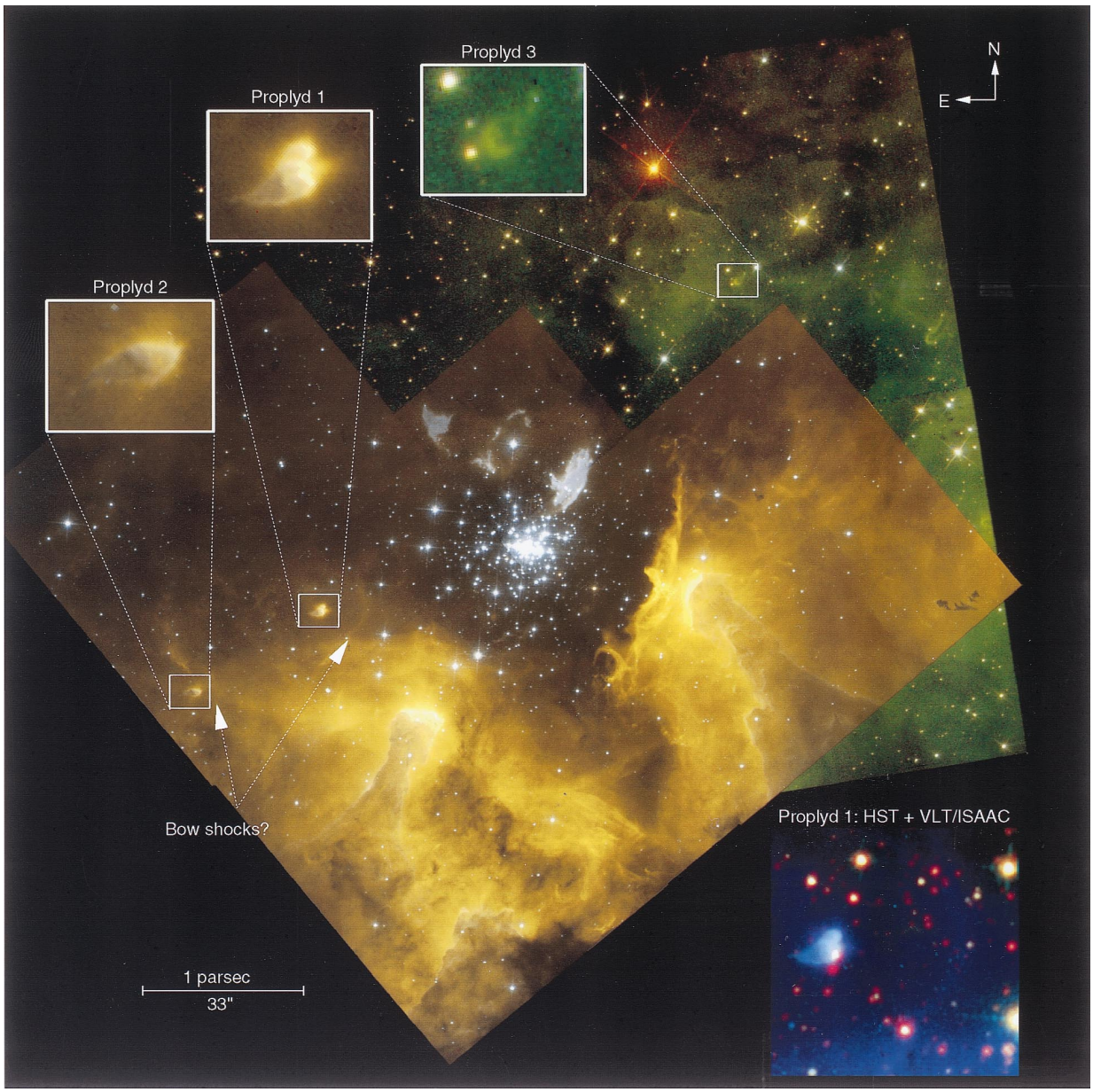

FIG. 1.—WFPC2 observations of NGC 3603. North is up and east is to the left. The upper part of the image consists of the archive data with the following color coding: F547M (*blue*), F675W (*green*), F814W (*red*). Overlaid are our new WFPC2 data with the F656N data in the red channel, the average of F656N and F658N in the green channel, and F658N in the blue channel. The location of the three proplyd-like emission nebulae is indicated. The insert at the lower right is a combination of WFPC2 F656N (*blue*) and F658N (*green*) and VLT/ISAAC K_s (*red*) observations.

All three proplyds are tadpole shaped and rim brightened, with the extended tails facing away from the starburst cluster. The portion of the ionized rims pointing toward the cluster is brighter than the rims on the opposite side. The central parts of the proplyds are fainter than the rims, with a noticeable drop in surface brightness between the head and the tail.

Proplyds 2 and 3 exhibit a largely axisymmetric morphology, whereas proplyd 1, which is also the one closest to the cluster, has a more complex structure. Unlike the convex shape of the heads of the other proplyds, proplyd 1 has a heart-shaped head with a collimated, outflow-like structure in between. One possible explanation for the more complex morphology of proplyd 1 might be that it is actually a superposition of two (or maybe even three) individual proplyds or that the photoevaporative flows of several disks in a multiple system interact to produce this complex single structure.

At distances of 7.″4 and 2.″9 from proplyd 1 and 2, respectively, faint arclike Hα emission features are seen on the WFPC2 frames. The arcs are located in the direction of the cluster, and may be the signatures of bow shocks created by the interaction of proplyd winds with the winds from the massive stars in the central cluster.

The proplyd heads have diameters between 1.″2 and 1.″7 (7200 and 10,800 AU). The head-to-tail extent of the proplyds is between 2.″5 and 3.″5 (15,000 to 21,000 AU). In Orion the typical diameters of the proplyd heads vary from 45 to 355 AU (O'Dell 1998), and the proplyd head in M8 has a diameter of 1080 AU (Stecklum et al. 1998). Thus, the proplyds in NGC 3603 are 20 to 30 times larger than the largest proplyds in Orion and 7 to 10 times larger than

TABLE 1

LOCATION AND SIZE OF THE THREE PROPLYD-LIKE STRUCTURES

Name	R.A.	Decl.	Distance from Cluster (arcsec)	Size
Proplyd 1.....	11 15 13.13	−61 15 50.0	43.6 (1.3 pc)	1.8[a] × 3.2
Proplyd 2.....	11 15 16.59	−61 16 06.2	72.5 (2.2 pc)	1.4 × 3.5
Proplyd 3.....	11 15 07.73	−61 15 16.8	68.0 (2.0 pc)	1.2 × 2.5

NOTE.—Units of right ascension are hours, minutes, and seconds, and units of declination are degrees, arcminutes, and arcseconds (2000.0).

[a] 0.″9, if we assume that proplyd 1 is a superposition of two or three individual proplyds.

the proplyd in M8. It should be noted that proplyds with sizes similar to those of the Orion proplyds would be too small to be resolvable at the distance of NGC 3603, where one pixel (0.″1) on the wide field CCDs of WFPC2 corresponds to 600 AU. The PC data with a finer pixel scale of 0.″0456 pixel^{-1} (270 AU) reveal indeed several faint point sources, which appear to be brighter in Hα than in [N II]. A detailed analysis of these sources will be subject of a later paper (Grebel et al. 2000).

In Orion, the size of the proplyds loosely scales with distance from the ionizing source in the sense that proplyds further away from Θ^1 Ori C are larger (McCullough et al. 1995; Johnstone et al. 1998, O'Dell 1998). In NGC 3603, there is no such correlation between the size of a proplyd and its projected distance from the cluster. If, however, the complex structure of proplyd 1 results from multiple photoevaporating disks as discussed above, the size estimates based on isolated proplyds cannot be applied. Only if proplyd 1 can actually be decomposed into individual, isolated proplyds with diameters around 0.″9, would there be a tendency for increasing proplyd size with increasing distance from the cluster.

Coordinates, distance from the cluster center, and approximate size of the proplyds are given in Table 1.

3.2. *Surface Brightness of Proplyds*

The WFPC2 observations reveal that only the outermost layer of proplyd 1 is ionized, whereas the interior remains neutral. Table 2 gives the Hα flux and the surface brightness of the proplyds as measured from the WFPC2 frames. No Hβ observations were available, which would have allowed us to determine the extinction toward the proplyds based on the Balmer decrement. Literature values for the fore ground extinction toward NGC 3603 range from $A_v = 4$ mag to 5 mag (Moffat 1983; Melnick, Tapia, & Terlevich 1989). The Hα flux has thus been corrected for an assumed foreground extinction of $A_{H\alpha} = 4$ mag. The values for the surface brightness have not been corrected for extinction.

Proplyds in Orion get fainter with increasing distance from the ionization source. Proplyd 2 is about a factor of 2.8 fainter than proplyd 1. If the projected separation from the cluster center is comparable to the physical distance, then proplyd 2 should receive a factor of $(72.″5/43.″6)^2 = 2.8$ fewer UV photons than proplyd 1. The remarkably good agreement between the number of infalling UV photons and the brightness of the proplyd suggests that both proplyds are ionization bounded and receive most of the ionizing UV photons directly from the cluster.

Proplyd 3 was only observed with intermediate and broadband filters. Its red colors ($V-R = 3.26$ mag, $R-I = 0.67$ mag) are caused by a combination of the absence of any strong emission lines in the passband of the F547M filter, foreground extinction, and possibly the presence of an embedded central continuum source.

Results from the VLT near-infrared broadband photometry can be found in Table 3. The surface brightness of all three proplyds increases from J_s to H to K_s. The photometry for proplyds 1 and 3 has not been corrected for the contamination by the nearby point sources.

3.3. *Nearby Point Sources*

The deep near-infrared observations with the VLT reveal a large number of faint, red point sources. Two point sources are detected close to the head of proplyd 1. As can be seen in the lower right insert of Figure 1, one of the point sources coincides with the location of the ionization front and may be physically associated with proplyd 1. Its red near-infrared colors (see Table 3) indicate that the source is highly embedded and/or has a strong intrinsic IR excess. This is in agreement with what one would expect for a young stellar object (YSO) surrounded by a circumstellar disk and an infalling envelope. Comparing with theoretical pre–main-sequence evolutionary tracks by Palla & Stahler (1993), we note that a 1 Myr old YSO with $J = 15.4$ mag and located in NGC 3603 should have a mass around 3 $M_\odot$ (Eisenhauer et al. 1998; Brandl et al. 1999). The effects of additional local extinction and accretion luminosity would of course alter this value. In any case it should be kept in mind that the relatively high density of field sources makes

TABLE 2

SURFACE BRIGHTNESS OF PROPLYD HEADS[a]

Name	$I_{H\alpha}$[b] (cm^{-2} s^{-1})	Hα (mag arcsec^{-2})	[N II] (mag arcsec^{-2})	F547M (mag arcsec^{-2})	F675W (mag arcsec^{-2})	F814W (mag arcsec^{-2})
Proplyd 1.....	0.56	13.60	15.90	...	...	...
Proplyd 2.....	0.20	14.73	16.71	...	...	...
Proplyd 3.....	...	...	...	24.84	21.58	20.91

[a] In Hα (F656N), [NII] (F658N), V (F547M), R (F675W), and I (F814W), measured for a 0.″5 aperture radius in the *HST* VEGAMAG system.

[b] Flux corrected for an assumed foreground extinction in Hα of $A_{H\alpha} = 4$ mag.

TABLE 3
VLT/ISAAC DATA

Name	J_s	H	K_s
Near-infrared surface brightness:			
Proplyd 1 (mag arcsec^{-2}).....	14.8	13.7	12.9
Proplyd 2 (mag arcsec^{-2}).....	16.2	15.7	14.5
Proplyd 3 (mag arcsec^{-2}).....	14.0	12.8	12.2
Photometry of nearby point sources:			
Proplyd 1 (mag)	15.4	14.1	13.4
Proplyd 3 (mag)	12.9	13.2	12.6

the physical association between this point source and proplyd 1 somewhat uncertain.

The point source close to the head of proplyd 3 is already detected on the broadband *HST*/WFPC2 observations (see Fig. 1). The WFPC2 images show that the point source is actually located in front of proplyd 3 and thus very likely not physically associated with it.

The J_s, H, and K_s magnitudes of the point sources associated with proplyd 1 and 3 can also be found in Table 3. No central point source is detected in proplyd 2 with a limiting magnitude of $K_s \leq 18.0$ mag.

3.4. *Optical Spectroscopy*

Figure 2 shows the low-resolution spectrum of proplyd 1. The most prominent emission lines are identified. If one assumes an electron temperature of 10^4 K, which is quite typical for H II regions, the flux ratio between the [S II] lines at 671.7 nm and at 673.1 nm yields an electron density well in excess of 10^4 cm^{-3}. Unfortunately, such densities are close to the collisional deexcitation limit of the [S II] doublet, which prevents us form getting a more precise estimate. Other density indicators such as the extinction corrected Hα surface brightness or the ratio of the [C III] UV doublet would have to be employed in order to derive a more accurate estimate of the density (see Henney & O'Dell 1999). Densities of the order of 10^5 cm^{-3} to 10^6 cm^{-3} have been found in the Orion proplyds (Henney & O'Dell 1999) and are also typical for Ultra Compact H II regions.

The infrared source in proplyd 1 is also detected as an underlying, heavily reddened continuum source in the spectrum. A more detailed analysis of ground based optical images and spectra of the proplyds and other compact nebulae in NGC 3603 will be presented in Dottori et al. (2000).

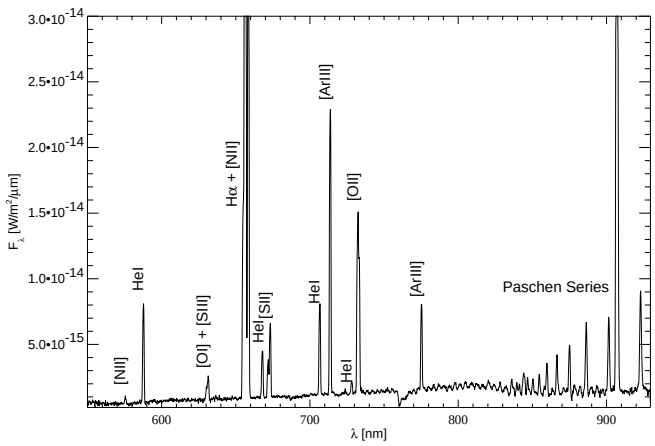

FIG. 2.—Spectrum of proplyd 1. The most prominent emission lines have been marked. The rising continuum toward longer wavelengths indicates the presence of an embedded continuum source.

3.5. *Limit on the Radio Brightness*

The proplyds in Orion have also been detected with the Very Large Array as radio continuum sources at 2 cm and 20 cm (Churchwell et al. 1987; Felli et al. 1993; McCullough et al. 1995).

NGC 3603 has recently been studied with the Australia Telescope Compact Array (ATCA) at 3.4 cm radio continuum and at several recombination emission lines (De Pree et al. 1999). Down to the 5 σ level of 55 mJy beam^{-1} for a beam size of 7″ none of the proplyds are detected in the continuum.

Following the derivation by McCullough et al. (1995; § 5), the expected ratio between the radio flux density due to Bremsstrahlung and the Hα flux is

$$\frac{F_{\rm radio}}{I_{\rm H\alpha}} = 3.46 \nu_{\rm GHz}^{-0.1} T_4^{0.55} \frac{\rm mJy}{\rm photons\ cm^{-2}\ s^{-1}},$$

where $\nu_{\rm GHz}$ is the radio frequency in GHz and T_4 is the electron temperature of the ionized gas divided by 10,000 K.

Thus, for the Hα flux values given in Table 2 and $T_4 = 1$, one would expect 3.4 cm (8.8 GHz) radio flux densities of 1.6 mJy and 0.55 mJy for proplyds 1 and 2, respectively. This is well below the detection limit of the ATCA observations by De Pree et al. (1999). Internal absorption of Hα photons emitted from the far side of the proplyd amounts to on average less than 25% to the total flux (McCullough 1993) and has thus been neglected in the above estimate.

These analytical estimates are in good quantitative agreement with the results from the numerical simulations described in § 5.

4. ENVIRONMENT

4.1. *UV Radiation Field*

NGC 3603, containing over 20 O stars and WR stars, creates a much more extreme UV environment than the Trapezium system. The central cluster in NGC 3603 has a Lyman continuum flux of 10^{51} s^{-1} (Kennicutt 1984; Drissen et al. 1995), about 100 times the ionizing power of the Trapezium system.

At the same time, however, the proplyds in NGC 3603 are at larger distances from the ionizing source. The projected separations between the proplyds and the cluster center range from 1.3 pc to 2.2 pc. The separation between Θ^1 Ori C and the Orion proplyds studied by O'Dell (1998) varies between 0.01 pc and 0.15 pc. On average, the proplyds in NGC 3603 are exposed to a somewhat less intense EUV ($h\nu \geq 13$ eV) radiation field than the proplyds in Orion.

The most massive stars in NGC 3603 are O3V stars and WR stars (Moffat, Drissen, & Shara 1994; Drissen et al. 1995), which are of earlier spectral type than the late O stars in the Trapezium system. As a consequence, the spectral characteristics of the UV field in NGC 3603 are different from those of the UV field in Orion. The early O-type stars in NGC 3603, although more luminous than the late O-type stars in the Trapezium system, produce a disproportionate smaller rate of FUV (13 eV $> h\nu \geq 6$ eV) photons compared to the rate of EUV photons. Table 4 gives the ratio of the FUV to EUV photon rates for blackbodies with temperatures between 30,000 K and 45,000 K. Model calculations of the atmospheres of hot stars made available in

TABLE 4

RATIO OF FUV TO EUV PHOTON RATES

$T_{\rm eff}$ (K)	BLACKBODY	STELLAR PHOTOSPHERE[a]	
		$Z = 0.2\ Z_\odot$	$Z = Z_\odot$
30,000.....	4.9	45.5	130
35,000.....	3.1	6.4	6.9
40,000.....	2.2	2.3	2.4
45,000.....	1.6	1.7	1.4

[a] Derived from stellar photosphere models by Pauldrach et al. (1998).

electronic form by A. Pauldrach[12] (see also Pauldrach et al. 1998) indicate that for effective temperatures below 45,000 K the ratio of FUV to EUV photon rates is considerably higher than the ratio derived for a blackbody. The models indicate ratios of 6.9:1 and 2.4:1 for O dwarfs with solar metallicity for effective temperatures of 35,000 K and 40,000 K, respectively (see Table 4).

Because all the EUV photons get absorbed in the ionization front, the FUV photon rate determines the heating inside the proplyd envelope and thus ultimately the mass-loss rate (Johnstone et al. 1998).

4.2. *Winds and Mass-Loss Rates*

Another important constituent of the environment of massive stars are fast stellar winds and wind-wind interactions. In Orion, four of the five proplyds closest to Θ^1 Ori C show arclike features which may be bow shocks resulting from the interaction of the evaporation flow of the proplyds with the fast stellar wind from Θ^1 Ori C (McCullough et al. 1995). The WFPC2 observations in Hα of NGC 3603 reveal similar arclike features in front of proplyds 1 and 2, which might also be bow shocks.

For a stationary shock, pressure equilibrium exists on both sides of the shock:

$$P = \rho_{\rm cl}(r_{\rm cl})v_{\rm cl}^2 = \rho_{\rm pr}(r_{\rm pr})v_{\rm pr}^2 ,$$

where $\rho(r)$ is the density of the wind at a distance r from the cluster (cl) or the proplyd (pr), respectively, and v is the terminal velocity of the freely expanding wind.

If radiative cooling is not important, the stagnation point of the shock along the line connecting the cluster with the proplyd relates to $\dot{M}v$ like

$$\frac{\dot{M}_{\rm cl}\, v_{\rm cl}}{\dot{M}_{\rm pr}\, v_{\rm pr}} = \frac{r_{\rm cl}^2}{r_{\rm pr}^2} ,$$

where $\dot{M}$ is the mass-loss rate of the cluster and the proplyd, respectively (e.g., Kallrath 1991).

Mass-loss rates of individual O stars in NGC 3603 are of the order of a few $10^{-7}\ M_\odot\ {\rm yr}^{-1}$, and wind velocities are of the order of a few 1000 km s^{-1} (Pauldrach et al. 1998). If we assume that the 20 O and WR stars in NGC 3603 have average mass-loss rates of $3 \times 10^{-7}\ M_\odot\ {\rm yr}^{-1}$, and average wind velocities of v = 2000 km s^{-1}, the resulting rate of momentum input $\dot{M}v$ from the combined winds would be $0.012\ M_\odot\ {\rm yr}^{-1}\ {\rm km\ s}^{-1}$.

The separation between the arc in front of proplyd 1 and the cluster center is 36.″2, and the separation between the arc and the proplyd is 7.″4. For a bow shock, the ratio between the product of mass-loss rate times the velocity of the wind from the cluster and proplyd 1 would thus be 24:1.

For a wind velocity of the evaporation flow from proplyd 1 of, e.g., 25 km s^{-1}, the mass-loss rate would then have to be $2 \times 10^{-5}\ M_\odot\ {\rm yr}^{-1}$. Whereas this is somewhat on the high end of the parameter space (see section on radiation hydrodynamical simulations below), the arclike feature between proplyd 1 and the cluster could indeed be the result of a bow shock. It should be kept in mind, however, that the mass-loss rates for the WR stars in NGC 3603 are highly uncertain, and might be considerably higher than our present estimate.

For proplyd 2 the separation between the arc and the proplyd is 2.″9, and the separation between the arc and the cluster center is 69.″6. Hence the ratio between the product of mass-loss rate times the velocity of the wind from the cluster and proplyd 2 is 580:1, which requires much less extreme conditions. For example, a mass-loss rate of $2 \times 10^{-6}\ M_\odot\ {\rm yr}^{-1}$ and a wind velocity of 10 km s^{-1} would balance the wind force from the cluster at a distance of 2.″9 from proplyd 2. Such values are in the range of mass-loss rates and flow velocities observed for the proplyds in Orion (e.g., Henney & O'Dell 1999; Bally et al. 1998b).

5. RADIATION HYDRODYNAMICAL SIMULATIONS

The proplyds in NGC 3603 are much larger than the proplyds in Orion. In order to investigate whether the proplyds in NGC 3603 can be explained by a similar physical mechanism as the proplyds in Orion, we carried out radiation hydrodynamical simulations.

5.1. *Numerical Method and Initial Conditions*

The simulations are based on a two-dimensional radiation hydrodynamics code (Yorke & Welz 1996; Richling & Yorke 1997, 1998; Richling 1998) and include a thin disk with a finite scale height. Diffuse EUV and FUV radiation fields are treated in the flux-limited diffusion approximation (Levermore & Pamraning 1981) as implemented for multiple nested grids by Yorke & Kaisig (1995). The present simulation utilizes 6 nested grids with a resolution from 7.3 AU to 233 AU The coarsest outermost grid covered a cylindrical volume of radius 13,500 AU and height 27,000 AU

The radial and vertical density structure of the disk was derived from the collapse of a rotating molecular cloud core with a mass of 2 $M_\odot$. The collapse was followed up through 5×10^5 yr, at which time 1.14 $M_\odot$ had already been accreted by the central protostar, while 0.86 $M_\odot$ still remained in the protostellar disk and the infalling envelope. Angular momentum transport was considered via an α-prescription (Shakura & Sunyaev 1973), as described by Yorke & Bodenheimer (1999). The inclusion of the effects of angular momentum transport is important, as disk material in the outer region of the disk actually gains angular momentum during the evolution, which results in a very extended disk.

The resulting initial disk had a diameter of 3400 AU This might seem large compared to the typical disk sizes observed for the proplyds in Orion. Based on their numerical models, Johnstone et al. (1998) derive disk sizes between 27 AU and 175 AU for the proplyds in Orion.[13]

[12] http://www.usm.uni-muenchen.de/people/adi/adi.html.

[13] Note that the disk radii r_d given by Johnstone et al. (1998) are actually in units of 10^{14} cm, not in units of 10^{17} cm as erroneously quoted in the column heads of Table 1 and 2 in their paper.

TABLE 5

MODEL PARAMETERS

Parameter	Value
Distance to ionizing source	4.01×10^{16} m (1.3 pc)
$T_{\rm eff}$	38,500 K
Luminosity	$2.02 \times 10^{7}\ L_{\odot}$
EUV flux ($h\nu \geq 13.6$ eV)	10^{51} s^{-1}
FUV flux (6 eV $\leq h\nu <$ 13.6 eV)	1.2×10^{52} s^{-1}

For disks that do not show any sign of external illumination by UV photons, typical disk sizes are in the range of 200 to 1000 AU (McCaughrean & O'Dell 1996; Padgett et al. 1999). It suggests that the extreme UV radiation field in the Trapezium cluster is evaporating the disks away at a rapid pace. This is in agreement with the small remnant disk masses and high mass-loss rates and is supported by the evaporation timescales of the order of 10^4 yr computed by Henney & O'Dell (1999). One would expect that larger disks also lead to the formation of more extended proplyds. Larger disks could be the result, e.g., of an initially higher angular momentum in the collapsing molecular cloud core.

With the aim to simulate the physical conditions close to those observed in NGC 3603 for proplyd 1, the EUV photon rate was set to 10^{51} photons s^{-1}, and the distance to the ionizing source to 4.01×10^{16} m (1.3 pc). The effective temperature of the central source was set to 38,500 K and the bolometric luminosity to $2.02 \times 10^{7}\ L_{\odot}$.

We carried out two sets of simulations for different FUV photon rates. For the first set the FUV photon rate was determined from a blackbody spectrum. As indicated in Table 4, this leads to an underestimate of the true FUV photon rate and results in lower mass-loss rates and a smaller size of the proplyd. For the second set of simulations the FUV photon rate was set to 1.2×10^{52} photons s^{-1}. In the following we will discuss only the results from the second set of simulations. The initial conditions for this set of simulations are summarized in Table 5.

5.2. *Mass-Loss Rates and Life Expectancy*

Figure 3 shows the evolution of the proplyd with time from the instant the Lyman continuum flux was turned on. An ionization front engulfing the star-disk-envelope system develops almost instantaneously. Initial mass-loss rates of the order of $10^{-5}\ M_{\odot}$ and evaporation flow velocities of the order of 20 km s^{-1} lead to a rapid depletion of the central mass reservoir. After 50,000 yr the disk-envelope system has already lost two-thirds of its initial mass. After 100,000 yr only 0.1 $M_{\odot}$ remains in the disk. After 140,000 yr almost 95% of the disk mass has been evaporated.

The simulations confirm the finding by Johnstone et al. (1998) that the FUV photon rate drives the mass-loss by heating up the region between the embedded disk and the ionization front. The resulting neutral flow influences the size of the ionized envelope. The simulations agree well with timescale estimates for disk photoevaporation by Hollenbach, Yorke, & Johnstone (2000).

5.3. *Emission-Line Maps in Hα*

In an attempt to compare the model to our *HST* observations, we computed the emission-line maps in Hα. The map shown in Figure 4 is based on the numerical model at a time of 50,000 yr. A viewing angle of 60° was assumed. The map was convolved with a theoretical *HST*/WFPC2 point-spread function computed with TinyTim (Krist & Hook 1997) and then resampled to the resolution of the Planetary Camera.

Overall, the simulated Hα map shows a good resemblance to the observations, and the models provide a viable explanation for the proplyds in NGC 3603.

Despite the high FUV photon rate, the resulting proplyd is still a factor of two smaller than the proplyd-like structures observed in NGC 3603. This would indicate that either the central disks are larger or that the proplyds in NGC 3603 have only very recently (within the last 10^4 yr) been exposed to the UV radiation field. The latter would cause timescale problems as it would require a very rapidly receding H I/H II front.

6. SUMMARY AND OUTLOOK

While the present analysis cannot give a definite answer about the nature of the proplyd-like nebulae in NGC 3603, the WFPC2 data already provide a number of important clues:

1. The tadpole shape suggests that the dynamics of the proplyds are dominated by the central cluster of NGC 3603.
2. The variation of the Hα brightness of the proplyds with distance to the ionizing cluster further indicates that the proplyds are ionization bounded.
3. The *HST*/WFPC2 and VLT/ISAAC images nicely resolve the nebulae into a region of neutral material surrounded by an outer ionization front. As discussed by O'Dell (1998), the fact that proplyds are ionization bounded implies that no EUV photons, but only FUV photons, penetrate and heat up the central region of the proplyds. The neutral interior provides a steady supply of material for the ionization front.
4. The key to a better understanding of the internal density structure of the nebulae is the direct detection of central point sources, such as the source possibly associated with proplyd 1. The near-infrared photometry alone, however, does not really allow for a good estimate of the overall luminosity of the embedded source and the amount of internal extinction. Similarly, the limited spectral resolution of our ground-based spectra does not allow us to determine mass-loss rates for the proplyds.
5. Faint nebular arcs detected between the proplyds and the cluster can be explained by bow shocks resulting from the interaction of the evaporation flow with the winds from the high-mass stars in the cluster.

The simulations indicate that high mass-loss rates of the order of $10^{-5}\ M_{\odot}$ yr^{-1} are necessary in order to explain the physical size of the proplyds. Similar to the Trapezium system, the proplyd-like structures in NGC 3603 appear to be short-lived phenomena. The fact that we detect three proplyds in NGC 3603 then suggests that proplyds/circumstellar disks are common not only in Orion but throughout the Milky Way.

Another consequence of the short life expectancy of proplyds in giant H II region is that they are not likely to survive long enough to form planetary systems, which are expected to form on timescales of the order of 10^6 yr (Lissauer 1987). It might, however, also be possible to form giant planets on a considerably shorter timescale (Boss 1998).

While we do not have definite proof that the proplyd-like

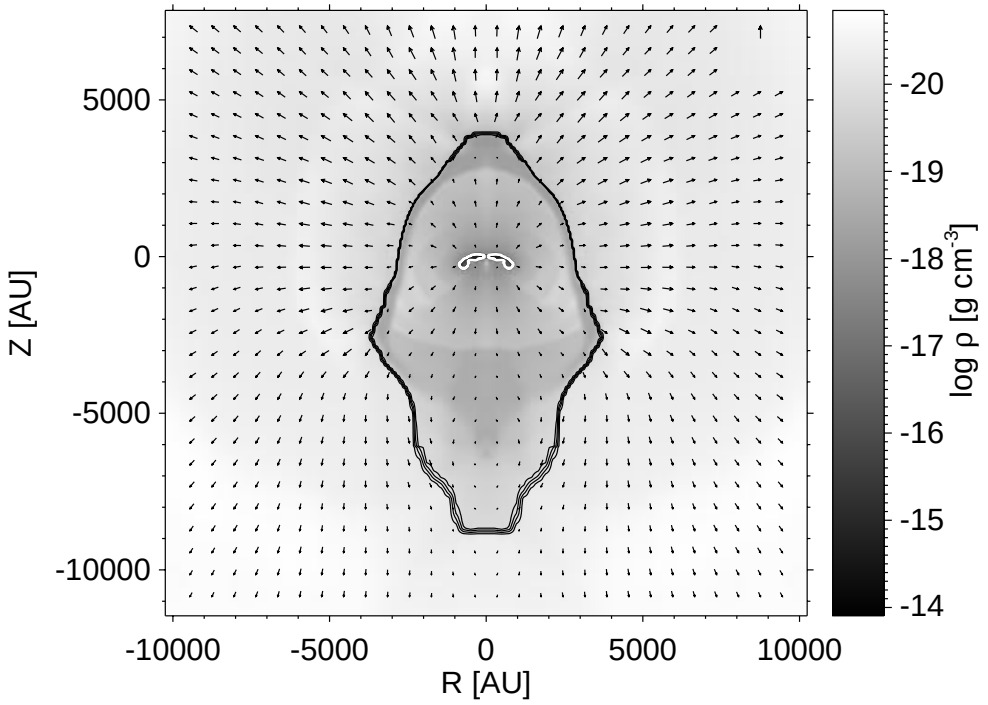

FIG. 3*a*

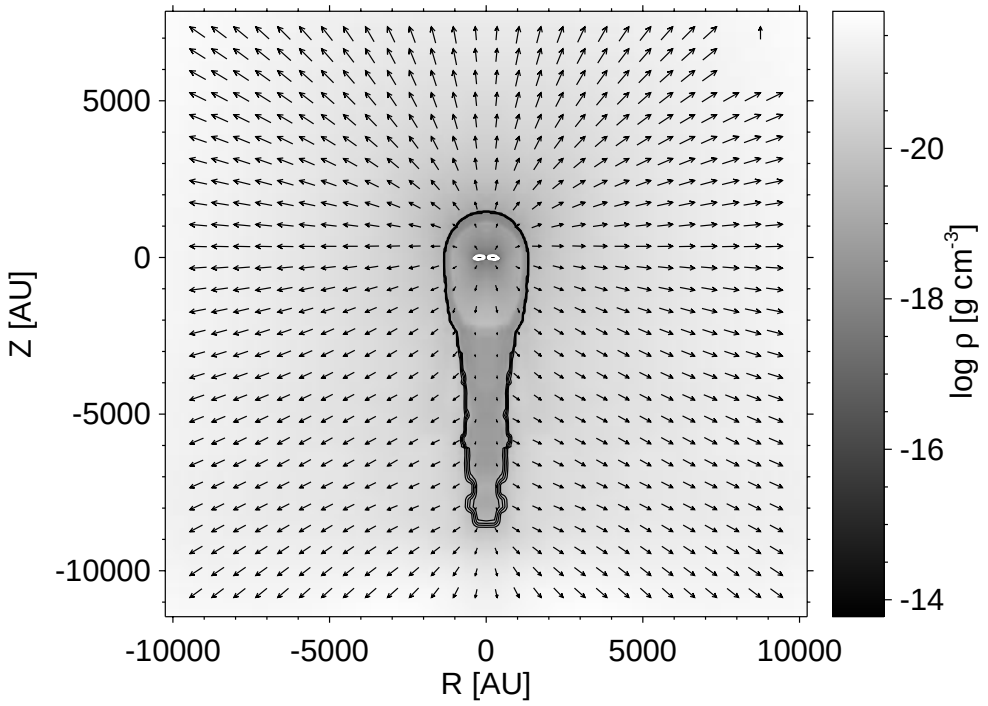

FIG. 3*b*

FIG. 3.—Time evolution of a proplyd based on two-dimensional radiation hydrodynamic simulations. The plots show the density distribution and evaporation flow velocity field at $t = 2416$ yr (*a*), $t \approx 50{,}000$ yr (*b*), and $t \approx 138{,}000$ yr (*c*). The disk can be seen as the light structure (*high density*) in the center of each plot. The ionization front is indicated by the dark solid line. Despite an initial mass of 0.8 $M_\odot$ in the disk and infalling envelope, the evaporation flow with a mass-loss rate of $10^{-5}\ M_\odot\ \mathrm{yr}^{-1}$ results in an almost complete evaporation of the disk within $\approx 10^5$ yr.

features in NGC 3603 are of the same nature as the proplyds in Orion, the similarities in morphology and physical characteristics strongly suggest that they are related phenomena. The numerical modeling shows that the proplyds can indeed be scaled to the size and the physical conditions in NGC 3603.

Further observations are needed to elucidate the nature of the proplyd-like nebulae in NGC 3603. High spatial resolution imaging and spectroscopy with *HST* in the optical and near-infrared will provide additional insights. Similar to Orion, it might be possible to detect the central disks glowing in the optical [O I] emission line and in the

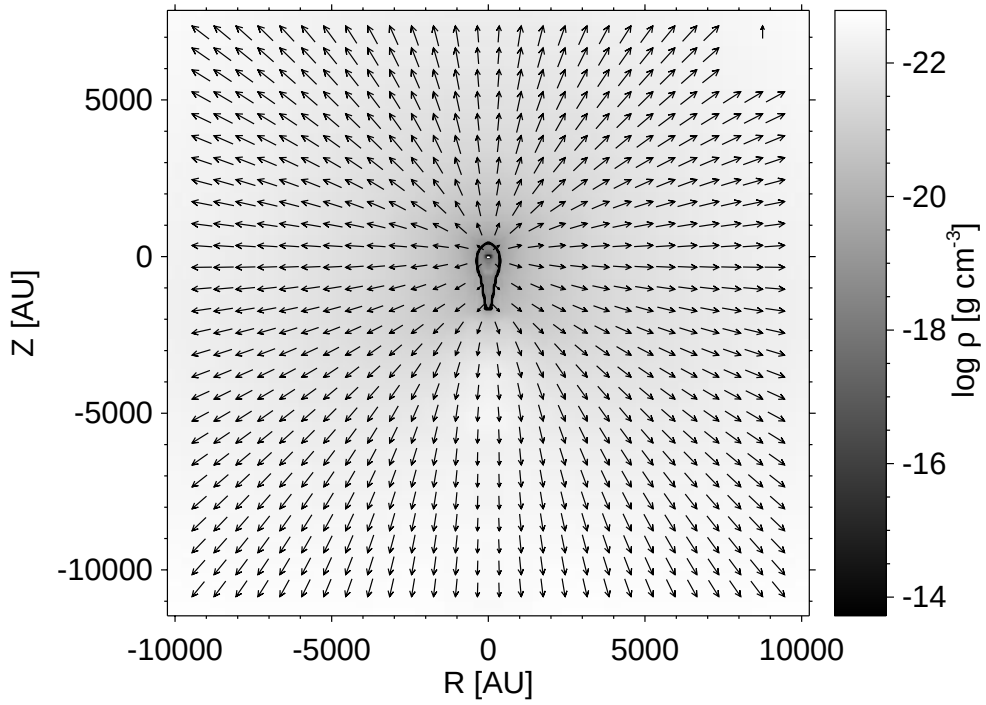

FIG. 3*c*

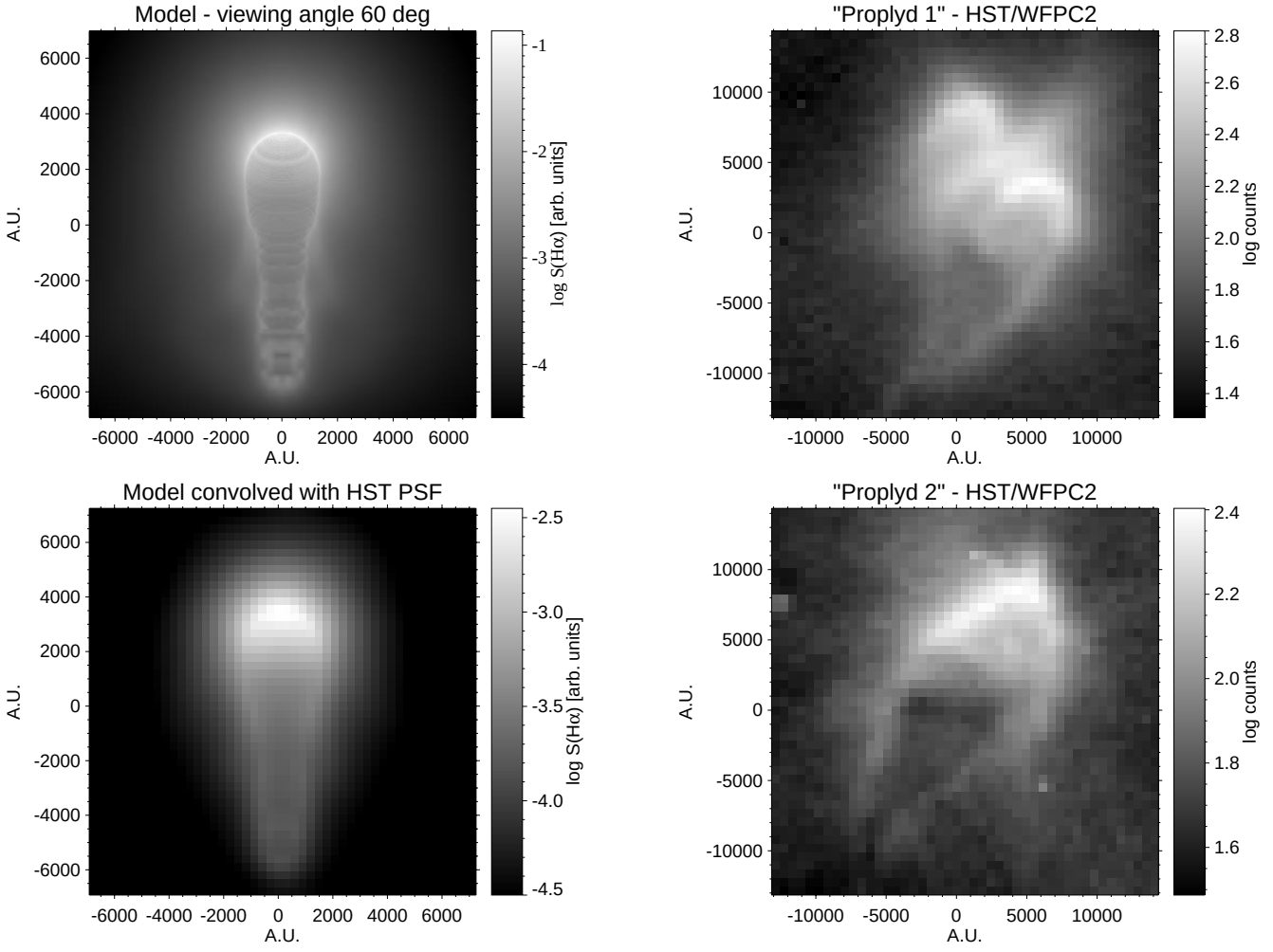

FIG. 4.—Comparison of an Hα emission-line map of the 50,000 yr old model and observed proplyds. The model has been convolved with a TinyTim point-spread function (Krist & Hook 1997) and resampled to the pixel scale of the Planetary Camera.

near-infrared molecular hydrogen lines. The physical extent, location within the proplyd, and inclination of the disk would provide important constraints for the simulations.

While the radio continuum survey by De Pree et al. (1999) at 3.4 cm did not detect the proplyds, in the future it might be possible to detect and resolve the disks with the Atacama Large Millimeter Array (ALMA), which is currently under study for the Chilean Atacama desert.

Deep ground-based thermal infrared imaging with the new generation of 6 to 8 m–class telescopes in the southern hemisphere could lead to the detection of more heavily embedded protostars in the center of the proplyds. The luminosity of each protostar would provide important constraints on its mass and evolutionary status.

This research is supported by NASA through grant GO 07373.01-96A from the Space Telescope Science Institute, which is operated by the Association of Universities for Research in Astronomy, Inc., under NASA contract NAS 5-26555. Part of this research has been carried out at the Jet Propulsion Laboratory (JPL), California Institute of Technology, and has been supported by NASA through the Origins program. The calculations were performed on computers operated by the Rechenzentrum der Universität Würzburg, the JPL/Caltech Supercomputing Project, and the John von Neumann Institute for Computing in Jülich. E. K. G. acknowledges support by NASA through grant HF 01108.01-98A from the Space Telescope Science Institute. Y. H. C. acknowledges the NASA grant NAG 5-3246. H. D. acknowledges support by a fellowship from the Alexander-von-Humboldt-Foundation. We would like to thank Robert Gruendl for helpful discussions and comments and the anonymous referee for the fast reply and the helpful comments and suggestions.

REFERENCES

Bally, J., Testi, L., Sargent, A., & Carlstrom, J. 1998b, AJ, 116, 854
Bally, J., Yu, K. C., Rayner, J., & Zinnecker, H. 1998a, AJ, 116, 1868
Boss, A. P. 1998, ApJ, 503, 923
Brandl, B., Brandner, W., Moffat, A., Eisenhauer, F., Palla, F., & Zinnecker, H. 1999, A&A, 352, L69
Brandner, W., Chu, Y.-H., Eisenhauer, F., Grebel, E. K., & Points, S. D. 1997a, ApJ, 489, L153
Brandner, W., Grebel, E. K., Chu, Y.-H., & Weis, K. 1997b, ApJ, 475, L45
Churchwell, E., Felli, M., Wood, D. O. S., & Massi, M. 1987, ApJ, 321, 516
De Pree, C. G., Nysewander, M. C., & Goss, W. M. 1999, AJ, 117, 2902
Dottori, H., et al. 2000, A&A, submitted
Drissen, L., Moffat, A. F. J., Walborn, N. R., & Shara, M. M. 1995, AJ, 110, 2235
Eisenhauer, F., Quirrenbach, A., Zinnecker, H., & Genzel, R. 1998, ApJ, 498, 278
Felli, M., Churchwell, E., Wilson, T. L., & Taylor, G. B. 1993, A&AS, 98, 137
Grebel, E. K., Brandner, W., & Chu, Y.-H. 2000, in preparation
Henney, W. J., & O'Dell, C. R. 1999, AJ, 118, 2350
Hollenbach, D., Yorke, H. W., & Johnstone, D. 2000, in Protostars and Planets IV, ed. V. Mannings, A. Boss, & S. Russell (Tucson: Univ. Arizona Press), in press
Hunt, L. K., Mannucci, F., Testi, L., Migliorini, S., Stanga, R. M., Baffa, C., Lisi, F., & Vanzi, L. 1998, AJ, 115, 2594
Johnstone, D., Hollenbach, D., & Bally, J. 1998, ApJ, 499, 758
Kallrath, J. 1991, MNRAS, 248, 653
Kennicutt, R. C. 1984, ApJ, 287, 116
Krist, J., & Hook, R. 1997, The TinyTim User's Handbook, Version 4.4 (Baltimore: STScI)
Laques, P., & Vidal, J. L. 1979, A&A, 73, 97
Levermore, C., & Pomraning, G. 1981, ApJ, 248, 321
Lissauer, J. J. 1987, Icarus, 69, 249
McCaughrean, M. J., & O'Dell, C. R. 1996, AJ, 111, 1977
McCullough, P. R. 1993, Ph.D. thesis, Univ. California, Berkeley
McCullough, P. R., Fugate, R. Q., Christou, J. C., Ellerbroek, B. L., Higgins, C. H., Spinhirne, J. M., Cleis, R. A., & Moroney, J. F. 1995, ApJ, 438, 394
Melnick, J., Tapia, M., & Terlevich R. 1989, A&A, 213, 89
Moffat, A. F. J. 1983, A&A, 124, 273
Moffat, A. F. J., Drissen, L., & Shara, M. M. 1994, ApJ, 436, 183
Moorwood, A., et al. 1998, Messenger, 94, 7
O'Dell, C. R. O. 1998, AJ, 116, 1346
O'Dell, C. R. O., Wen, Z., & Hu, X. 1993, ApJ, 410, 686
O'Dell, C. R. O., & Wong, S.-K. 1996, AJ, 111, 846
Padgett, D. L., Brandner, W., Stapelfeldt, K. R., Strom, S. E., Terebey, S., & Koerner, D. 1999, AJ, 117, 1490
Palla, F., & Stahler, S. W. 1993, ApJ, 418, 414
Pauldrach, A. W. A., Lennon, M., Hoffmann, T. L., Sellmaier, F., Kudritzki, R.-P., & Puls, J. 1998, in ASP Conf. Ser. 131, Properties of Hot, Luminous Stars, ed. I. Howarth (San Francisco: ASP), 258
Persson, S. E. Murphy, D. C., Krzeminski, W., Roth, M., & Rieke, M. J. 1998, AJ, 116, 2475
Richling, S. 1998, Ph.D. thesis, Julius-Maximilians-Univ. Würzburg
Richling, S., & Yorke, H. W. 1997, A&A, 327, 317
———. 1998, A&A, 340, 508
Shakura, N. I., & Sunyaev, R. A. 1973, A&A, 24, 337
Stapelfeldt, K. et al. 1997, in ASP Conf. Ser. 119, Planets beyond the Solar System and the Next Generation of Space Missions, ed. D. Soderblom (San Francisco: ASP), 131
Stecklum, B., Henning, T., Feldt, M., Hayward, T. L., Hoare, M. G., Hofner, P., & Richter, S. 1998, AJ, 115, 767
Störzer, H., & Hollenbach, D. 1999, ApJ, 515, 669
Yorke, H. W., & Bodenheimer, P. 1999, ApJ, 525, 330
Yorke, H. W., & Kaisig, M. 1995, Comput. Phys. Comm., 89, 29
Yorke, H. W., & Welz, A. 1996, A&A, 315, 555